

THE INFLUENCE OF THE HEAT-TREATMENT REGIME ON A FRACTURE SURFACE OF NICKEL-BASED SUPERALLOYS

VPLIV TOPLOTNE OBDELAVE NA POVRŠINO PRELOMA SUPERZLITIN NA OSNOVI NIKLJA

**Andjelka Milosavljevic¹, Sanja Petronic², Suzana Polic-Radovanovic³,
Jasmina Babic⁴, Darko Bajic⁵**

¹Faculty of Mechanical Engineering, Belgrade, Serbia

²Innovation Center of the Faculty of Mechanical Engineering, Belgrade, Serbia

³Central Institute for Conservation, Belgrade, Serbia

⁴Military Technical Institute, Belgrade, Serbia

⁵Faculty of Mechanical Engineering, Podgorica, Montenegro
sanjapetronic@yahoo.com

Prejem rokopisa – received: 2012-01-11; sprejem za objavo – accepted for publication: 2012-02-23

Nickel-based superalloys are distinguished from other materials by their excellent mechanical and physical properties. As they are used at high temperatures and pressures, as well as in aggressive environments, their characteristics need constant improvement. An adequate choice of their chemical composition and the heat-treatment regime contributes to the improvement of the chemical, physical and mechanical properties of these nickel-based superalloy materials. During the heat treatments of the superalloys Nimonic 263 and Hastelloy S some changes in their microstructures were observed. In this paper the changes in the microstructures after various regimes of the heat treatment were analysed on the fractured surfaces. The fractured surfaces were observed using light microscopy, scanning electron microscopy (SEM), and energy-dispersive X-ray spectrometry (EDS).

Keywords: superalloy, heat treatment, microstructure, EDS, SEM

Superzlitine na osnovi niklja se razlikujejo od drugih materialov zaradi svojih odličnih mehanskih in fizikalnih lastnosti. Ker se jih uporablja pri visokih temperaturah in tlakih ter v agresivnem okolju, je potrebno stalno izboljševati njihove lastnosti. Primerna izbira kemijske sestave in načina toplotne obdelave prispevata k izboljšanju kemijskih, fizikalnih in mehanskih lastnosti superzlitine na osnovi niklja. Med toplotno obdelavo superzlitine Nimonic 263 in Hastelloy S se opazijo spremembe v mikrostrukturi. V tem članku so analizirane spremembe mikrostrukture na prelomnih površinah po različnih toplotnih obdelavah. Površina prelomov je bila opazovana s svetlobno mikroskopijo, vrstično elektronsko mikroskopijo (SEM) in rentgensko disperzijsko spektroskopijo (EDS).

Ključne besede: superzlitina, toplotna obdelava, mikrostruktura, EDS, SEM

1 INTRODUCTION

Modern industry has a high demand for superalloys due to their enhanced technological features, such as good mechanical strength and hardness, corrosion resistance, heat resistance, wear resistance and surface degradation¹⁻³.

The good tensile strength of superalloys is based on the principle of a stable face-centered cubic matrix combined with precipitation hardening and/or solid-solution strengthening⁴.

Precipitation hardening produces a high strength with finely dispersed precipitates formed during the heat treatment and deposited in the elastic matrix. These particles can be obstacles to the movement of dislocations through the crystal structure, thus reinforcing the heat-treated alloy.

The effect of the superalloys' strengthening depends on the type of particles. The best results can be achieved when the coherent and partially coherent particles finely disperse within the matrix.

Precipitation hardening increases the mechanical properties, especially the strength of the materials, with the precipitation from supersaturated solid solutions. The principal strengtheners in the nickel-based superalloys are complex precipitates of γ' [$\text{Ni}_3(\text{Al}, \text{Ti})$] and γ'' [$\text{Ni}_3(\text{Nb}, \text{Al}, \text{Ti})$] and the carbide particles. Other phases have a negligible effect on increasing the tensile strength, but a significant effect on increasing the creep and fracture strength, and the segregation⁵.

Some unwanted phases can precipitate during the heat treatment, plastic deformation and/or long-time service. By selecting the optimal heat-treatment time and the optimal heat-treatment temperature, these phases could be avoided^{5,6}.

In addition, a proper selection of the chemical composition and the heat treatment contributes to an improvement of the chemical, physical and mechanical properties of the nickel-based superalloys⁷.

During the heat treatment of the superalloys Nimonic 263 and Hastelloy S the phase transformations occurred⁸.

The influence of the heat treatment on the microstructure of various metals and their alloys has been

investigated so far^{5,9-12}, but, bearing in mind the importance and applicability of these superalloys in industry, it is undoubtedly important to further investigate the influence of heat treatment on the microstructure of these superalloys.

In this paper, the influence of heat treatment on the microstructure of two nickel-based superalloys, which have been strengthened with different strengthening mechanisms, is investigated. Hastelloy S is a solid-solution strengthened alloy with a high content of molybdenum. Nimonic 263 is a precipitation-hardenable alloy with an addition of molybdenum for the solid-solution strengthening. These two superalloys are very often used in domestic industry.

2 EXPERIMENTAL

In this paper, the experimental investigations are carried out on the commercial, nickel-based superalloys Nimonic 263 and Hastelloy S. The samples are cut from the sheets, thickness of 1.2 mm. The chemical composition is determined by the gravimetric method and listed in **Table 1**.

The homogenization heat treatment of the superalloys Nimonic 263 and Hastelloy S is performed in a vacuum at a temperature of 1050 °C and for 16 h, with the aim to achieve a homogeneous structure.

The samples of Nimonic 263 superalloy are subjected to a two-stage heat treatment:

- 1) solid solution at 1150 °C and cooling in water,
- 2) aging at 800 °C/8 h and cooling the air.

The solid solution time at a temperature of 1150 °C for one group of Nimonic 263 samples is 10 min (regime – R1). As the results obtained after regime R1 suggest that the solid-solution time is short, the second group of samples is subjected to a solid solution treatment for 60 min (regime – R2), due to the assumption that longer periods of solid solution treatment could bring about the formation of coarse particles. The regime of precipitation hardening for both groups is the same – 800 °C/8 h cooled air.

The heat treatment of the superalloy Hastelloy S, described according to literature data and experience^{5,13}:

- Solution treatment at 1080 °C/1 h and rapidly cooled in water to room temperature,
- Primary precipitation hardening at 840 °C/4 h and cooling to room temperature,
- Secondary precipitation hardening at 760 °C/3 h and cooling in air to room temperature.

After the heat treatment carried out according to the described regime, the superalloy samples were prepared for light microscopy. After the polishing of the samples the etching was performed for the superalloys Nimonic 263 and Hastelloy S in a solution with the following composition: 30 % H₂O, 20 % HNO₃, 10 % HF, 20 % H₃PO₄ and 10 % CH₃COOH.

The fractured surfaces were observed with a light microscope (model KEYENCE VH-Z100), a scanning electron microscope (model JOEL JSM-5800) and analysed using energy-dispersive X-ray spectrometry.

The tensile tests were performed with a mechanical universal testing machine (Schenck-Trebel, RM400) and the 0.2 % offset yield strength, tensile strength and elongation were determined. The tensile tests were carried out at room temperature according to the en 10002-1 standard. The hardness tests were made with a semi-automatic Hauser 249A and the HV₃₀ was measured.

3 RESULTS AND DISCUSSION

The first step in the heat treatment of superalloys is usually a solid-solution treatment. The solid-solution temperature depends on the required characteristics.

Higher temperatures are used for optimum creep-fracture properties, and produce a higher yield and a more extensive carbide dissolution. Lower temperatures result in the optimal yield strength at elevated temperature and a resistance to fatigue¹⁴.

By observing the microstructure of the Nimonic 263 samples, prepared for light microscopy by polishing and etching, at 225-times magnification, there is a difference in grain size, i.e., a finer grain size is achieved for the heat treatment regime R2 (**Figure 1b**) than for the heat-treatment regime R1 (**Figure 1a**). The average grain size is calculated using the method of the circle¹⁵ and their values are as following: $F_m = 314.78 \mu\text{m}^2$ and $F_m = 237.68 \mu\text{m}^2$ for the regimes R1 and R2 applied, respectively.

The values measured by Vickers hardness with a load of 30 N are:

- HV₃₀ = 283 regime R1,
- HV₃₀ = 302 for regime R2.

The finer grain structure and the higher hardness values imply that the heat treatment carried out by regime R2 has a more favourable impact on the properties of the superalloy Nimonic 263, compared to the heat treatment by regime R1.

After the heat treatment, regime R2, which was preceded by homogenization, the microstructure of the

Table 1: Chemical composition of Nimonic 263 and Hastelloy S superalloys in mass fractions (w/%)

Tabela 1: Kemijska sestava superzlitin Nimonic 263 in Hastelloy S v masnih deležih (w/%)

Element	C	Si	Mn	Al	Co	Cr	Cu	Fe	Mo	Ti	Ni
Nimonic 263	0.06	0.3	0.5	0.5	20	20	0.1	0.5	5.9	2.2	49.94
Hastelloy S	0.3	0.5	0.5	0.3	–	15.3	–	1.34	14.4	–	67

Table 2: Results of EDS-analysis of the spectrums in **Figure 2a** (w/%)

Tabela 2: Rezultati EDS-analize spektrov s **slike 2a** (w/%)

Spectrum	Al	Si	Ti	Cr	Mn	Fe	Co	Ni	Mo
Spectrum 1	0.2	0.11	1.99	32.42	0.32	0.25	13.87	44.82	6.02
Spectrum 2	0.22	0.21	6.73	19.35	0.34	0.26	17.82	49.25	5.82
Spectrum 3	0.51	0.28	2.01	19.89	0.5	0.48	20	50.4	5.93
Spectrum 4	0.47	0.32	2.2	20.03	0.46	0.52	20.32	49.85	5.83
Spectrum 5	0.54	0.27	2.18	19.95	0.53	0.51	19.98	50.14	5.9

superalloy Nimonic 263 consists of the following: γ solid solution, γ' intermetallic compounds – γ' [Ni₃(Al, Ti)], carbides M₂₃C₆, MC carbide and a number of annealing twins. The volume fraction of γ' for the start of the thermal deposition is about 10 %¹⁶, and its fraction increases with the deposition time, and is unevenly distributed in the γ solid solution. The M₂₃C₆ carbides are densely distributed at the grain boundaries, while the amount of MC carbide is small and mainly formed during solidification and precipitation. The MC carbides are mainly Ti carbides, and Ti is a γ' former as well. This explains the creation of γ' -free zones at the grain boundaries, as Ti forms carbides, and depletes Ti in the γ solid solution near the grain boundaries.

Figure 2a shows a micrograph of the microstructure of superalloy Nimonic 263, after heat treatment – the regime R2. The results of the EDS analysis are listed in **Table 2**. It is clear that the Cr and Ti carbides precipitate

at the grain boundaries, which confirms the increased content of Cr in spectrum 1 and the increased content of Ti in spectrum 2. An analysis of the grain (spectrums 3, 4, 5) indicates that the chemical composition is generally close to the average one. For chromium carbides we could not exactly determine the type of carbide. According to the literature^{3,5,17,18} they could be the M₂₃C₆ type carbide, which are densely distributed at the grain boundaries. The size of these carbides is up to 600 nm. Their shape is elliptical, and they are uniformly distributed at the grain boundaries. The size, morphology, distribution and location of these carbides are favourable for the straightening of superalloy. Comparing to¹⁶ where time of the solid solution was shorter, these carbides are finer and more uniformly distributed at the grain boundaries.

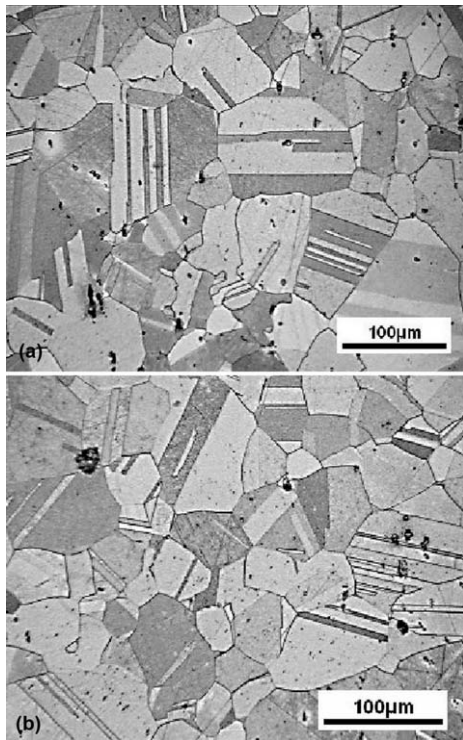


Figure 1: The microstructure of the superalloy Nimonic 263 after heat treatment by: a) regime R1, b) regime R2, taken with an optical microscope

Slika 1: Mikrostruktura superzlitine Nimonic 263 po toplotni obdelavi: a) način R1, b) način R2, optični mikroskop

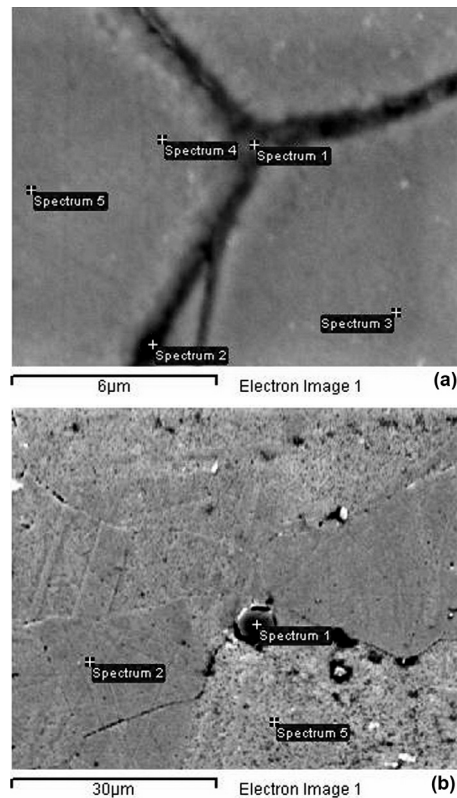


Figure 2: a) Carbides precipitated at the grain boundaries after the heat treatment regime R2, b) TiC carbide precipitated by solution treatment of regime R1 (SEM)

Slika 2: a) Karbidni izločki po mejah zrn po toplotni obdelavi z načinom R2, b) TiC karbidni izločki po raztopnem žarjenju po načinu R1 (SEM)

Table 3: Results of EDS analysis of the spectrums in **Figure 2b** (w/%)

Tabela 3: Rezultati EDS-analize spektrov s **slike 2b** (w/%)

Element	Al	Si	Ti	Cr	Mn	Fe	Co	Ni	Mo
Spectrum 1	–	–	80.99	3.83	–	–	0.35	14.83	–
Spectrum 2	0.34	0.35	2.32	18.9	0.29	0.47	19.95	51.28	6.1
Spectrum 3	0.44	0.38	18.58	16.15	0.29	0.52	15.15	48.49	–

Table 4: Results of EDS analysis of the spectrums in **Figure 3** (w/%)

Tabela 4: Rezultati EDS-analize spektrov s **slike 3** (w/%)

	Al	Si	Ti	Cr	Mn	Fe	Co	Ni	Mo
area in Fig. 3.a)	0.45	1.33	2.80	19.88	0.90	0.52	17.72	49.04	6.47
Spec1–Fig. 3.b)	0.47	0.48	8.79	19.13	0.39	0.80	16.40	46.17	6.37
Spec2–Fig. 3.b)	0.58	0.63	7.30	20.34	0.28	0.48	17.47	46.60	6.31

According to **Figure 2b** and **Table 3**, it can be concluded that in spectrum 1, at the grain boundaries, the carbide TiC precipitated. The grain boundaries are γ' -free, and the EDS analysis in spectrum 3 and **Figure 2b** indicates that Ti carbides are deposited at the grains. It is believed that this is the reason for the relatively small amount of γ' phase. The carbides at the grains are fine and considered as being favourable for the strengthening of the structure.

However, the Ti carbide in spectrum 1 is due to the short time of the solution treatment, and then the rapid cooling. It is considered to be too large to be beneficial

to the microstructure. The carbide is hexagonal, up to 6.15 μm in size, and locally precipitated at the triple grain boundary. Due to its size, this carbide can be a convenient place for the deposition of a topologically close-packed (TCP) phase, and may be the initiator of the appearance of microcracks.

The characterization of the microstructural changes of the fracture surfaces occurring in the stated superalloys for the regimes R1 and R2 was made by scanning electron microscopy and energy-dispersive X-ray spectrometry analysis, as shown in **Figures 3** and **4**.

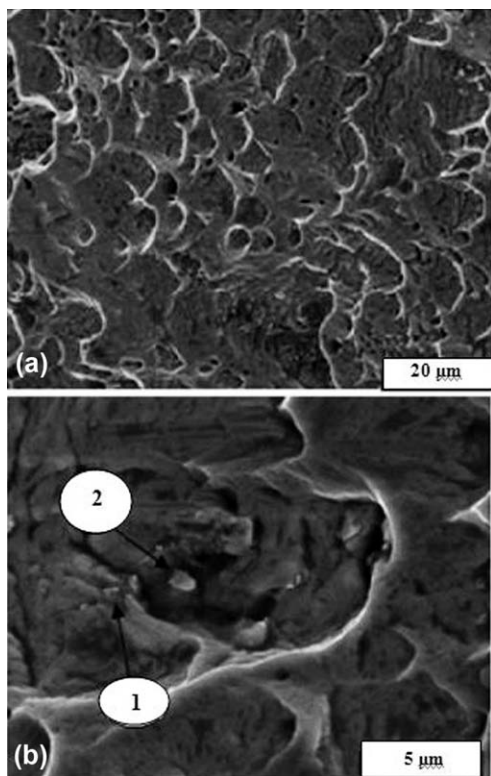


Figure 3: a) The appearance of a fracture surface after the heat treatment R2, b) carbides at the fracture surface

Slika 3: a) Videz površine preloma po toplotni obdelavi z načinom R2, b) karbidi na površini preloma

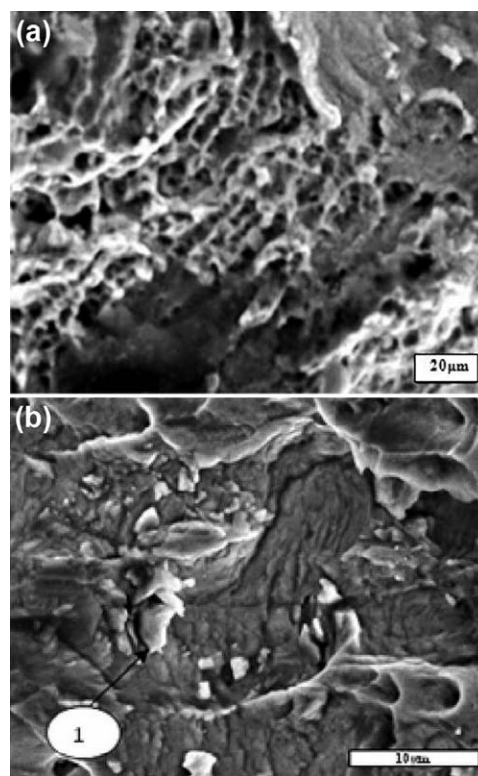


Figure 4: a) The appearance of a fracture surface of the Nimonic 263 superalloy after heat treatment R1, b) detail from **Figure 4a** – unfavourable Ti carbide

Slika 4: a) Videz površine preloma superzlitine Nimonic 263 po toplotni obdelavi z načinom R1, b) detajl s **slike 4a** – nezaželeni Ti-karbidi

Table 5: Results of EDS-analysis of the spectrums in **Figure 4** (w/%)

Tabela 5: Rezultati EDS-analize spektrov s **slike 4** (w/%)

	Al	Si	Ti	Cr	Mn	Fe	Co	Ni	Mo
The area in Fig. 4.a)	0.25	1.33	2.80	19.88	0.90	–	17.72	51.04	6.47
Spectrum 1 – Fig. 4.b)	–	–	46.55	12.01	0.51	0.21	10.20	28.47	2.16

Table 6: Results of EDS-analysis of the area in **Figure 6a** (w/%)

Tabela 6: Rezultati EDS-analize področja s **slike 6a** (w/%)

	Al	Si	Cr	Mn	Fe	Ni	Mo
Whole area in Fig. 6a	0.4	0.46	14.86	0.54	1.08	64.82	18.6
Whole area in Fig. 6b	0.38	0.48	15.04	0.56	1.33	65.41	17.8

Table 7: Mechanical properties of superalloys Nimonic 263 and Hastelloy S after applied heat treatments

Tabela 7: Mehanske lastnosti toplotno obdelanih zlitin Nimonic 263 in Hastelloy S

Mechanical properties	$R_{0.2} / (N/mm^2)$			$R_m / (N/mm^2)$			$A_5 / (%)$		
	I	II	III	I	II	III	I	II	III
Nimonic 263 R1	550	573	545	820	835	832	39	38	39
Nimonic 263 R2	582	587	593	972	975	979	39	40	39
Hastelloy S	464	450	466	845	839	837	49	48	50

The fractured surfaces were obtained from the tensile tests and the results of the tensile strength, yield strength (0.2 % offset) and elongation, together with the results obtained for the superalloy Hastelloy S, are given in **Table 7**.

Figures 3a and **3b** show the fracture surfaces of the superalloy Nimonic 263, after the heat treatment with

regime R2. The fractured surface is relatively homogeneous and the dimples are relatively uniform. In **Figure 3b** the same fracture is presented at a higher magnification. The deposition of Ti carbides can be observed, as confirmed by the EDS analyses listed in **Table 4**. The size of carbides is up to 1.16 μm and it is believed that these carbides are not the cause of the fracture.

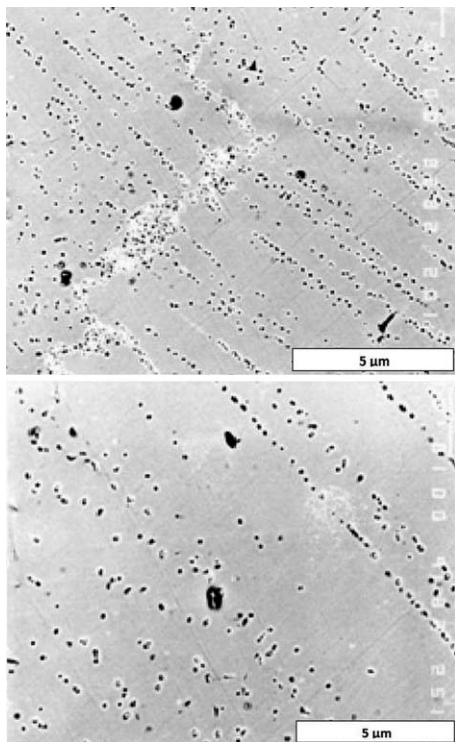


Figure 5: Molybdenum carbides precipitated in the superalloy Hastelloy S after heat treatment, taken with a light microscope

Slika 5: Karbidi molibdena, izločeni v toplotno obdelani superzlitini Hastelloy S; svetlobni mikroskop

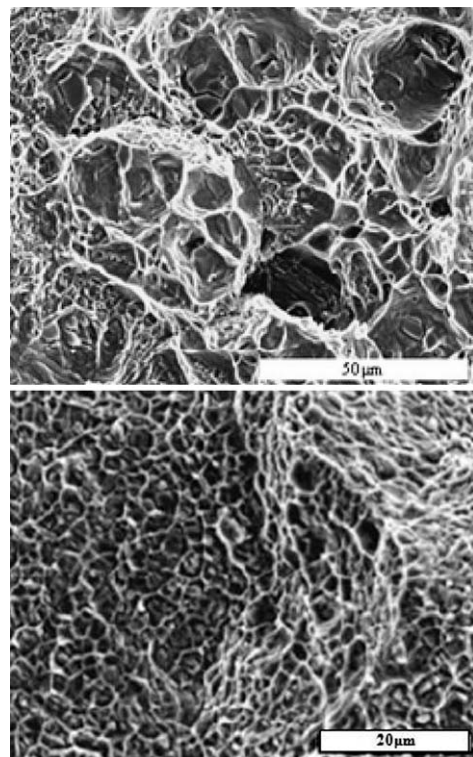


Figure 6: Fracture surfaces of the superalloy Hastelloy S taken with a SEM

Slika 6: Površina preloma superzlitine Hastelloy S (SEM)

Figures 4a and **4b** show the fractured surfaces of the Nimonic 263 superalloy after heat treatment – regime R1. In **Figure 4b** is a detail from **Figure 4a** – an unfavourable precipitated carbide. The EDS analysis results listed in **Table 5** confirm the assumption that it is a Ti carbide, and the place, morphology (irregular, hexagonal-like) and size (3.95 μm) suggest it has a negative influence on the mechanical characteristics of the material. It is believed that the large carbides contributed greatly to the breaking of the material.

Based on our observations of the samples of the superalloy Hastelloy S using a light microscope, the dark phases are visible, for which the energy-dispersive X-ray spectrometry analysis shows they are the molybdenum carbides. Their formation contributed the increased content of molybdenum in the alloy, as well, compared to the prescribed one.

The molybdenum carbides are segregated into arrays and nests – **Figures 5a** and **5b**. It is believed that these carbides, together with the Cr carbides that occur in these alloys, strengthened the alloy after the heat-treatment process.

Figures 6a and **6b** show the fractured surfaces of the superalloy Hastelloy S. In **Table 6** are the results of the EDS analysis of the whole areas presented in **Figure 6**. A higher content of molybdenum was observed, and this is consistent with light-micrograph analyses. The structure of the fractures is homogeneous and uniform, as confirmed by the EDS analysis conducted at the 150x and 5 000-times magnifications (**Table 6**). The chemical compositions of the two investigated surfaces differ very little, which implies the homogeneity of the structure.

The mechanical properties obtained with the tensile tests are listed in **Table 7**. Relatively high values of the tensile strength, the yield strength (0.2 % offset) and the elongation are in favour of a good heat treatment being applied. In this paper, the short-solid solution time (regime R1) results in lower values of the ultimate tensile strength and yield strength, while the elongation remains the same. The results listed in¹⁶, where the authors applied different aging times for three groups of samples, show that the various heat treatments have a large effect on all the tensile properties of the material. Compared to the literature data^{4,19} obtained for Nimonic 263 ($R_{0.2} = 580 \text{ MPa}$, $R_m = 970 \text{ MPa}$ and $A_5 = 39 \%$) we observed slightly higher $R_{0.2}$ and R_m values. According to the literature^{4,20} the tensile-test characteristics of the Hastelloy S alloy are: $R_{0.2} = 444 \text{ MPa}$, $R_m = 844 \text{ MPa}$ and $A_5 = 49 \%$. In this paper, the higher value of $R_{0.2}$, the yield strength (0.2 % offset), is obtained – the important characteristic of the material used in design projects. Based on the results in **Table 7**, the fracture appearance and the EDS analysis, it can be assumed that during the heat treatment the creation of undesirable phases has not taken place, which would help in the breaking of the material.

4 CONCLUSIONS

The microstructure and mechanical characteristics of the superalloys Nimonic 263 and Hastelloy S, besides processing route and chemical composition, depend to a large extent on the applied heat treatment. The heat-treatment processes of the superalloys Nimonic 263 and Hastelloy S, carried out according to the regimes described in this paper, indicate their considerable influence on the microstructure transformations, and in this way on the material properties. During the applied heat-treatment regimes, the various micro-constituents formed with a major influence on the properties of the materials.

The heat treatment of the superalloy Nimonic 263, which included 60 min of solid solution time (R2), rather than the 10 min solid solution time (R1), resulted in a better microstructure and better mechanical properties of the stated superalloy. During both regimes of heat treatment, Ti carbides participated, but according to the size, the morphology and the distribution in regime R2 they are favourable, while in regime R1 they are not. The grains are finer and more uniformly distributed after the heat treatment of regime R2 than after regime R1, i.e., with a longer solid-solution time. Also, the values of mechanical properties: the hardness, the ultimate tensile strength and the yield strength (0.2 % offset), are higher when the time of the solid solution treatment is longer.

After the heat treatment of the nickel-based superalloy Hastelloy S, applied in this study, the molybdenum carbides segregated. As a result, a higher value of the yield strength is obtained. This characteristic is critical in design projects, which makes these results very useful for engineering practice.

Acknowledgements

This work was supported by the Ministry of Science of the Republic of Serbia under contract number TR-35040 and TR 34028.

5 REFERENCES

- 1 R. C. Reed, *The Superalloys, Fundamentals and Applications*, 1st ed., Cambridge University Press, New York 2006, 163
- 2 C. T. Sims, W. C. Hagel, *The Superalloys*, Wiley-Interscience, New York 1972, 576
- 3 F. Tancret, H. K. D. H. Bhadeshia, D. J. C. MacKay, *Key Engineering Materials*, 171–174, (2000), 529–536
- 4 *Metal Handbook – Vol 1 & Vol 2, Properties and Selection: Iron, Steel, and High-Perf. Alloys*, 10th ed., ASM International, Materials Park, Ohio 2005, 2301
- 5 *Metal Handbook, Vol 4, Heat treating, Cleaning, Finishing*, 8th ed., ASM International, Metals Park, Ohio 1975, 1757
- 6 www.specialmetalswiggins.co.uk
- 7 V. Shankar, K. B. S. Rao, S. L. Mannan, *Journal of Nuclear Materials*, 288 (2001), 222–232
- 8 J. C. Zhao, V. Ravikumar, A. M. Beltran, *Metallurgical and Materials Transactions A*, 32 (2001), 1271–1282

- ⁹ J. X. Yang, Q. Zheng, X. F. Sun, H. R. Guan, Z. Q. Hu, *Materials Science and Engineering A*, 465 (2007), 100–108
- ¹⁰ W. Österle, S. Krause, T. Moelders, A. Neidel, G. Oder, J. Völker, *Materials Characterization*, 59 (2008), 1564–1571
- ¹¹ P. N. Singh, V. Singh, *Scripta Materialia*, 34 (2008) 12, 1861–1865
- ¹² R. Cahn, P. Haasen, *Physical Metallurgy*, 4th ed., Elsevier Science B. V., 1996, 1817
- ¹³ S. Petronic, A. Milosavljevic, *FME Transactions*, (2007) 35, 189–193
- ¹⁴ S. Zhao, X. Xie, G. D. Smith, S. J. Patel, *Materials Science and Engineering A*, 355 (2003), 96–105
- ¹⁵ H. Schumann, *Metallographie*, 9th ed., VEB Deutscher Verlag für Grundstoffindustrie – Leipzig, 1975, 41
- ¹⁶ W. Z. Wang, H. U. Hong, I. S. Kim, B. G. Choi, H. W. Jeong, M. Y. Kim, C. Y. Jo, *Materials Science and Engineering A*, 523 (2009), 242–245
- ¹⁷ X. Z. Qin, J. T. Guo, C. Yuan, C. L. Chen, J. S. Hou, H.Q. Ye, *Materials Science and Engineering A*, 485 (2008), 74 –79
- ¹⁸ H. M. Wang, L. G. Yu, X. X. Li, P. Jiang, *Science and Technology of Advanced Materials*, (2001), 173–176
- ¹⁹ <http://www.matweb.com/>
- ²⁰ <http://www.haynesintl.com/pdf/h3003.pdf>